World Academy of Science, Engineering and Technology
International Journal of Aerospace and Mechanical Engineering
Vol:9, No:2, 2015

A New Computational Tool for Noise Prediction of Rotating Surfaces (FACT)

Ana Vieira, Fernando Lau, João Pedro Mortágua, Luís Cruz, Rui Santos

Abstract—The air transport impact on environment is more than ever a limitative obstacle to the aeronautical industry continuous growth. Over the last decades, considerable effort has been carried out in order to obtain quieter aircraft solutions, whether by changing the original design or investigating more silent maneuvers. The noise propagated by rotating surfaces is one of the most important sources of annoyance, being present in most aerial vehicles. Bearing this is mind, CEIIA developed a new computational chain for noise prediction with in-house software tools to obtain solutions in relatively short time without using excessive computer resources. This work is based on the new acoustic tool, which aims to predict the rotor noise generated during steady and maneuvering flight, making use of the flexibility of the C language and the advantages of GPU programming in terms of velocity. The acoustic tool is based in the Formulation 1A of Farassat, capable of predicting two important types of noise: the loading and thickness noise. The present work describes the most important features of the acoustic tool, presenting its most relevant results and framework analyses for helicopters and UAV quadrotors.

Keywords—Rotor noise, acoustic tool, GPU Programming, UAV noise.

I. Introduction

THROUGHOUT the last decades, as aeronautical industry grew, aerial vehicles overran city skies, contributing to the already high levels of noise present in such populated areas. The negative effects of excessive levels of noise in the balance of human and animal life are well known, leading to restrictive noise pollution regulations which affect directly the aeronautical industry.

Rotating surfaces as rotors, propellers and fans are usually the most significant source of noise during flight, being its accurate prediction a key step in reducing the noise footprint on ground.

This type of noise source is particularly evident in rotorcraft, in which rotor noise is a major contribution to the overall noise level.

The decade of 60's was marked by the first theoretical and experimental studies about rotor noise generation, as well as the implementation of computer codes based on such theories. However, the lack of computer power and the limited understanding of the role of the blade surface pressure distribution did not allow great progresses.

A. Vieira is with the R&D Department, CEIIA, Portugal, (e-mail: ana.vieira@ceiia.com).
F. Lau is with the Aerospace Group, IST, Portugal.
J. P. Mortágua is with the R&D Department, CEIIA, Portugal.
L. Cruz is with the Aerodynamics Dep., CEIIA, Portugal.
R. Santos is with IN+, IST, Portugal.

The following decades were marked by major advances in theoretical formulations related to rotor noise prediction. One of the most important achievements was the derivation of the Ffowcs Williams-Hawkings equation in 1969 [1], where the Lighthill's acoustic analogy approach was generalized to include effects of general types of surface and motions. This great advance was followed by the emergence of the Kirchhoff formulation for moving surfaces [2] and the Farassat's Formulations 1 and 1A [3], which contributed for several computational codes of rotor noise prediction [4]–[6].

Recent years have been crucial in the development of more accurate and sophisticated rotorcraft noise prediction tools due to the evolution of computer power. However, there are still several issues that require further study in order to improve the noise prediction.

One of the most important subjects of study has been the rotor generated noise in maneuvering flight for complex geometries, which only recently began to be investigated [4], [5], [7]. The noise generated in maneuvering flight is still not completely addressed especially in the event of transient maneuvers [8], [9].

In comparison with other works related to this area, the main contribution of this computational tool is its flexibility, since the noise prediction can be performed to several rotorcraft configurations and flight conditions, including wind as atmospheric condition. The noise prediction in maneuvering flight, in particular, is still a relatively new field of research. In addition, the acoustic tool considers the movement of the whole rotorcraft, and not just of the rotors, separately, unlike many software tools.

Another contribution is the application of GPU programming to accelerate the simulation, which in the case of maneuvering flight and complex geometries can be a slow process.

The present work describes the new acoustic tool and analysis frameworks for helicopter and quadrotor UAV.

Helicopter noise has been extensively studied over the past decades, remaining a challenge even today due to its complex nature and massive computational resources required in its prediction.

In contrast, UAV noise is a recent field of study which is receiving more attention every day, not only because of eminent noise regulations, but also to extend its range of applications.

II. Theoretical Backgroung

This second section addresses the theoretical concepts used in the development of the acoustic tool, thus facilitating the comprehension of their application in the computational code.

A Nature of Rotor Noise

Rotor noise is composed by discrete-frequency and broadband noise components. The discrete-frequency noise contains the deterministic components of thickness, loading and high-speed impulsive (HSI) noise. Broadband noise comprehends non-deterministic loading noise sources like turbulence ingestion noise, blade-wake interaction and blade self-noise.

Thickness noise is generated by the fluid displacement originated by the blade motion and propagates along the rotor disk plane.

Loading noise results from the non-impulsive loading sources, generated by the accelerating force on the fluid as the blade is moving. Loading noise propagates in a direction below the rotor disk and it is usually the dominant source of rotor noise.

Blade-vortex interaction (BVI) noise is a specific type of loading noise generated by a very fast oscillation of the aerodynamic force on the blade surface as the result of an interaction between a shed tip vortex with the following blades. The BVI noise is the most significant noise source in approaching flight.

High-speed impulsive noise is generated when the rotor blade tips are at a Mach number superior to 0,85. HSI noise is significant in high-speed forward flight and propagates in the same direction as the thickness noise.

Broadband noise is related to turbulence and its current prediction methods are semi-empirical, depending on measured data to find the constants required in the model.

B Aeroacoustic Computational Chain

The acoustic analysis of a rotorcraft is a complex process, generally involving several software tools.

The computational chain developed at CEIIA comprises two in-house software tools: HFAST (Helicopter Full Aerodynamic Simulation Tool) and FACT (Farassat 1A Acoustic CEIIA Tool).

HFAST was adopted as the aerodynamic solver. The Free Wake Method implemented in HFAST is able to accurately represent the wake motion and its interaction with the lifting surfaces.

This software makes use of CUDA (Compute Unit Device Architecture) programming in order to accelerate the intense Free Wake routines. Additionally the wake can also be represented by segments of constant vorticity (CVC - Constant Vorticity Contours) which for the same precision is computationally less demanding and has automatic refinement in the regions with greater vorticity gradients.

HFAST is able to analyze the lifting surfaces of generic configurations, like helicopter, airplanes or wind turbines. The tool has specific control parameters for helicopters, like the rotor pitch controls and blade flapping, and some basic trimming capabilities, useful for performance analysis. The effects of viscosity, compressibility and Reynolds can be included through 2D profile C81 tables.

HFAST has been validated against comprehensive and well established helicopter aerodynamic analysis tools, providing similar result in a fraction of the time.

The acoustic solver FACT, presented in this paper, in its turn, converts the pressure fluctuations in the blade into the noise measured in a hemisphere of microphones below the rotorcraft.

C Formulation 1A of Farassat

Almost all actual rotor noise prediction tools are based on time-domain integral formulations of the Ffowcs Williams-Hawkings equation, being the Formulation 1A of Farassat one of them. The FW-H equation is based on the Lighthill's acoustic analogy and it is an exact rearrangement of the continuity equation and the Navier-Stokes equations into the form of an inhomogeneous wake equation. The FW-H equation is given by

$$\left(\frac{\partial^2}{\partial t^2} - c^2\frac{\partial^2}{\partial x_i^2}\right)(\overline{\rho-\rho_0}) = \frac{\partial}{\partial t}\left[\rho_0 v_n \delta(f)\right] - \frac{\partial}{\partial x_i}\left[p_{ij} n_j \delta(f)\right] + \frac{\partial^2 \overline{T}_{ij}}{\partial x_i \partial x_j}, \quad (1)$$

where $\overline{T}_{ij}$ is a generalized function equal to Lighthill's stress tensor $T_{ij} = \rho u_i u_j + p_{ij} - c^2(\rho-\rho_0)\delta_{ij}$ outside any surfaces and equal to zero within them. The speed of sound is represented as c, ρ is the fluid density, n_j is the normal vector to the surface, p_{ij} is the compressive stress tensor and v_n is the surface velocity in the normal direction.

The quadrupole term of (1) requires volume integration and an accurate prediction of the flow field, which involves large computational demands. For those reasons, the quadrupole term has been neglected in many tools of rotor noise prediction. Furthermore, the quadrupole source contribution is not significant in many subsonic applications, so it will be ignored from now on.

Therefore, only the solution of the following two wave equations is required,

$$\Box^2 p'_T = \frac{\partial}{\partial t}[\rho_0 v_n \delta(f)], \quad (2)$$

$$\Box^2 p'_L = -\frac{\partial}{\partial x_i}[l_i \delta(f)], \quad (3)$$

where p'_T and p'_L are the pressure perturbation due to the thickness and loading noise, respectively. $\delta(f)$ is the Dirac delta function, $l_i = p_{ij} n_j$ and $\Box$ is the D'Alembertian operator $\Box^2 = (1/c^2)(\partial^2/\partial t^2) - \nabla^2$.

Those two equations result into the following final

expressions for the thickness and loading noise:

$$p'_T(x,t) = \int_{f=0} \left[\frac{\rho_0 \dot{v}_n}{r(1-M_r)^2}\right] dS + \int_{f=0} \left[\frac{\rho_0 v_n}{r^2(1-M_r)^3}\left[r\dot{M}_r + c(M_r - M^2)\right]\right] dS\,, \tag{4}$$

$$p'_L(x,t) = \frac{1}{c}\int_{f=0} \left[\frac{\dot{l}_r}{r(1-M_r)^2}\right] dS + \frac{1}{c}\int_{f=0} \left[\frac{l_r(r\dot{M}_r + cM_r - cM^2)}{r^2(1-M_r)^3}\right] dS + \int_{f=0} \left[\frac{l_r - l_M}{r^2(1-M_r)^2}\right] dS\,. \tag{5}$$

In these two equations, all the variables are considered in the retarded time. The derivatives are in order of the retarded time, r is the radiation direction, M is the Mach number and S the area of the surface. The subscripts are related with the direction of the respective variable.

Brentner et al proved that the assumption of a chordwise compact loading distribution does not substantially affect the results of the loading noise [10]. Therefore, this formulation was adopted for the acoustic tool, since it is computer power saving and the distribution of the aerodynamic loading along the chordwise direction is often unavailable.

D Numerical Algorithms for Acoustic Integrals

Now that the choice of the formulation is set, it is necessary to adopt a numerical algorithm in order to implement the solution of the existing integrals. The formulation 1A of Farassat is a retarded-time formulation whose integrals can be solved through three different methods: the mid-panel quadrature, the high-accuracy quadrature and the source time-dominant algorithm.

The mid-panel quadrature method is the most common approximation. The surface is divided into N panels and the integral is evaluated at the center of each panel, defined at the retarded time. It is possible to build a history of p' through the choice of the observer time and position to each panel.

This approximation leads to good results when the panel size is sufficiently small because the retarded time value should not oscillate significantly over the panel and the source strength variation should be approximately linear.

The high-accuracy quadrature method is a refinement of the mid-panel quadrature method, since the evaluation of the integral at the panel center is replaced with more points. With a larger number of points, the limitations of the mid-panel quadrature method such as the nonlinearity of the source strength and the variation of the source time over the panel can be overcome. However, it is important to remember that more points imply more computational effort.

The previous two methods were based in a choice of the observer time a priori, however, an alternative to that process is to select the source time for a panel considering the central point y_i. This method is defined as a source time-dominant algorithm.

A consequence of this method is an unequally spaced history of observer time points which will require an interpolation procedure in order to sum the contribution of all panels in the same observer time.

One of the most important advantages of this algorithm is its convenience when the input data is provided by CFD analyses, since the time-dependent input data (availed at the source) does not need to be interpolated. Moreover, this algorithm is appropriate to parallel computation and requires significantly less operations for maneuvering rotor predictions than other algorithms. Since one of the aims of this project is to use parallel computation in order to accelerate the numerical operations, a source time dominant algorithm will be adopted.

E Wind Implementation

The original signal of noise propagated from rotating sources can be modified by several factors, for example, atmospheric effects and noise reflection.

The presence of wind is an inevitable atmospheric condition, which depending on its magnitude, might affect the noise perceived at the observer positions. However, the wind condition is equivalent to a uniformly moving media surrounding the rotor, and the Formulation 1A of Farassat considers that the medium is undisturbed.

Depending on the observer motion and the fluid speed, three distinct problems may be considered:

- **Fly-over**: both the observer and the ambient medium are stationary - the source can be stationary or moving;
- **Moving-observer**: the observer is moving (e.g. a microphone mounted in a fuselage) and the ambient medium is stationary;
- **Wind-tunnel**: the observer is stationary and the ambient fluid is moving.

The presence of wind is equivalent to the third case, a wind-tunnel configuration. In order to remain with the same acoustic analogy formulation, this problem can be transformed in a moving-observer case, i.e., the source and the observers are moving with the fluid velocity U_0, with the medium being stationary.

When the observer position x is stationary, the following equation must be solved in order to determine the instant the noise is received at the observer position:

$$t = \tau + \frac{|x - y(\tau)|}{c} \tag{6}$$

Here t stands for the observer time, τ for the source time, y for the source position and c for the speed of sound.

When the observer position is not stationary, (6) must be rewritten as represented in (7), meaning that the observer position is now time dependent.

$$t = \tau + \frac{|x(t) - y(\tau)|}{c} \tag{7}$$

So, both the observer position x and the observer time t have to be determined implicitly at the same time, and the solution ca be found by an iterative process. The method of Newton-Raphson was chosen to solver the present problem due to its efficiency.

F Signal Processing

A periodic signal can be approximated by a sum of sinusoids at the harmonic frequencies of the signal with appropriate amplitude and phase through a Fourier Transform. Applying this method, it is possible to go from the time domain to the frequency domain.

In this case, the signal is the acoustic pressure sampled over a finite time interval, so it will be used a Discrete Fourier Transform (DFT), defined by

$$X_p = \sum_{n=0}^{N-1} x_n e^{-j\frac{2\pi}{N}np} \quad , p \in \{0, 1, ..., N-1\}. \quad (8)$$

Here, a sequence of N numbers $x_0, x_1, ..., x_{N-1}$ is transformed into a N-periodic sequence of complex numbers $X_0, X_1, ..., X_{N-1}$.

The arithmetic operations necessary for the computation of the DFT are proportional to N^2 for an input sequence of length N, which demands large computational resources.

In 1965, Cooley and Tukey presented an alternative to the classic Fourier transform: the Fast Fourier Transform (FFT). The FFT only requires $Nlog_2(N)$ operations, which is an obvious advantage over the N^2 operations needed in the Fourier transform.

The core idea of this algorithm is the realization that a DFT of a sequence of N points can be written as two DFT of length $N/2$. Here it will be considered the most basic radix-2 algorithm which requires N to be a power of two. This is the simplest and most common form of the Cooley-Tukey algorithm and divides the DFT of size N into two DFTs. It is a recursive algorithm that rearranges the problem into two simpler problems with half the size.

Through the application of the FFT, the original signal is decomposed into sinusoids at its harmonic frequencies, with an appropriate value of amplitude and phase.

The result of the FFT is a sound spectrum where the amplitudes are sampled over the harmonics frequency, making it difficult to extract a physical meaning from the results. For this reason, both the amplitude and the frequency range shall be subjected to some manipulation.

In the original signal, the acoustic pressure, in Pascal (Pa), is sampled over a finite time interval, so, the amplitude obtained from the FFT is also in Pa. This unit of measurement is not the most adequate when dealing with noise levels due to its wide range of values.

Therefore, one can use a a logarithmic measure, designated as decibel (dB), created to the Sound Pressure Level (SPL), given by

$$SPL(dB) = 10\,log\left(\frac{p^2}{p_{ref}^2}\right) = 20\,log\left(\frac{p}{p_{ref}}\right), \quad (9)$$

where p_{ref} is a reference value equal to 2×10^{-5} Pa in the air.

The level of generated noise is subjective, so it is necessary to take into account the human ear, more sensitive in a range of 1 kHz to 5 kHz. The A-weighting decibel (dBA) was created to overcome this issue, being used as a noise scale in the present work.

It is impractical to analyze the signal frequency by frequency, so, the frequency range was divided into a set of frequencies, denominated as bands. Each one of those bands covers a certain range of frequencies, creating a scale of octave or one-third octave bands. The acoustic tool uses a scale of 1/3 octave bands, where the frequency range of 20 Hz to 20 kHz is divided into thirty-two 1/3 octave bands.

Another important parameter in noise analysis is the total energy contained in the spectrum, given by the Overall Sound Pressure Level (OASPL), where all the 1/3 octave bands are summed up.

G CUDA Programming

The GPU computing can be defined as the combination of a CPU with a GPU (Graphics Processing Unit), used to accelerate an application. GPUs were specially developed to accelerate and improve the efficiency of the code through the CPU. The CPU/GPU combination presents plenty advantages since a CPU consists of several cores specific for serial processing and a GPU is formed by thousands of cores suitable to parallel processing, allowing the separation of the code into different segments and sending them to CPU or GPU, according to its function (Fig. 1).

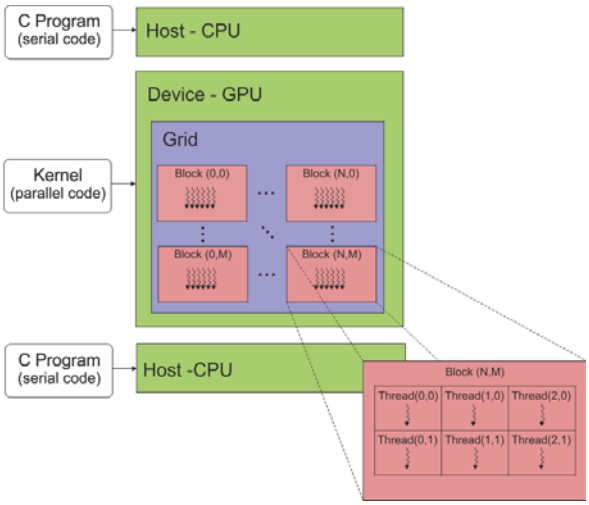

Fig. 1 Grid of microphones used in the simulation

One of the most popular and widespread language designed for parallel computing is NVIDIA®'s CUDA C, adopted in the present work.

III. Software Description

This section will be dedicated to the description of the software, thereby providing detailed information about the adopted concepts and assumptions.

A Input Specifications

FACT's input data is divided in three different categories:

- **Analysis parameters:** Air density, temperature, observer(s) position, number of iterations, iteration and

interpolation step, the type of movement (steady or unsteady flight) and wind velocity.

- **Input files:** which aerodynamic and mesh files would be used for each rotor blade;
- **Rotorcraft characteristics:** linear velocity, initial position, attitude, number of rotors, rotor position, tilt, flapping and pitching coefficients, number of blades and blade hinge position.

B Geometry and Aerodynamic Loading Parameters

The mesh input files generate the geometry of each blade in the rotorcraft, taking into account the thickness of the blade, essential to the thickness noise calculation.

The loading noise is correlated with spanwise integration, and thickness noise involves spanwise and chordwise integration, so, it is necessary to define two types of surfaces: panels and sections. A section is composed by several panels.

The computation of the thickness and loading noise requires, respectively, the calculation of several geometry parameters for each panel and section.

Therefore, it is necessary to calculate the central point, the area and the local coordinate system of each panel. The same parameters are required for each section, along with the calculation of the section span.

In the case of the loading input files, it is only necessary to keep the value of the aerodynamic force per unit length. EMMA exports the lift force generated in the blade, and the loading noise calculation requires the force applied on the blade, so, the saved values are symmetrical to the original ones.

C Implementation of the Helicopter Movement

FACT is capable of simulating steady flight and steady maneuvers. The user must specify the type of flight condition in the input file 'InputData.txt'. In the case of steady flight, the inputs presented into that file are considered the same in all iterations. If the helicopter is in maneuvering flight, the user must provide an additional input file called 'MOTION.case', containing the necessary values to the maneuver. Though the referred file, the user can choose which parameters change throughout the iteration: it is possible to change the rotorcraft linear velocity, the wind velocity, the rotor tilt, the angular velocity and the pitching and flapping coefficients.

Even before the beginning of the simulation of the helicopter movement, it is necessary to include the parameters introduced in the input file, in order to set correctly the position of the helicopter, rotors and blades.

First, all blades must be placed in its right initial azimuth position, ψ_0, considering that they are equally spaced. Therefore, it is possible to find the initial flapping and pitching angle of each blade, through (10) and (11), respectively.

$$\beta(\psi) = \beta_0 + \beta_{1c}\, cos(\psi) + \beta_{1s}\, sin(\psi)\,, \quad (10)$$

$$\theta(\psi) = \theta_0 + \theta_{1c}\, cos(\psi) + \theta_{1s}\, sin(\psi)\,. \quad (11)$$

Here, β_0 is the conning angle and β_{1s} and β_{1c} are, respectively, the amplitude of the pure sine and cosine of the flapping motion. θ_0 is the collective pitch, θ_{1c} is the longitudinal pitch and θ_{1s} is the lateral pitch.

The rotations inherent to the flapping and pitching angles are performed using the Rodrigue's Rotation Formula. The rotation of a blade implies the modification of several parameters and not just a rotation of the blade geometry: the blade local coordinate system, the hinge position, the central point and the local coordinate system of each section and panel also suffer rotations.

Now that all blades are in the correct flap and pitch positions, they are rotated about the central point of the rotor in order to set the right initial azimuth angle. Once again, it is necessary to rotate all the blade parameters referred above.

With all the blades in the right initial position, the next step is to apply the rotor initial conditions. The rotor tilt, comprising the tilting forward and sideways, is applied in the first place. In this regard, a rotor local coordinate system, moving and rotating with the rotor, was created. The procedure to calculate the rotor rotation originated by the tilt uses the same logic adopted in the blade rotation. This means that both the rotor local coordinate system and all blades and their respective parameters are rotated.

Besides the rotation, the rotors also need to be positioned in the correct position relatively to the helicopter, which implies a translation of the rotor origin and of the blades, resulting in an offset of the hinge position and central points of each panel and section.

At last, the rotorcraft initial conditions must be considered, namely the attitude and the initial position.

In order to implement the rotorcraft attitude, another auxiliary local coordinate system, moving with the helicopter, was defined. All the rotorcraft structures (rotors and blades) are rotated according to the pitch, yaw and roll angles, so all the previously mentioned parameters must be changed once again. The rotorcraft local coordinate system and origin are also updated.

Finally, the rotorcraft is placed in its initial position, which implies another translation of all the points constrained in its geometry.

With the rotorcraft geometry placed in the right position, all that is left is the calculation of the velocity of each rotor surface.

The linear velocity of each panel is simply the linear velocity of the rotorcraft. The rotation velocity, so named because of its origin (the angular velocity of the rotors), is given by

$$\overrightarrow{v}_{rot} = (\omega\, \overrightarrow{n}_z) \times (\overrightarrow{r}_{pnlCP} - \overrightarrow{r}_{rotorOrg})\,. \quad (12)$$

Here $\overrightarrow{v}_{rot}$ is the rotational velocity of each panel, ω is the rotor angular velocity, $\overrightarrow{n}_z$ is the rotor local coordinate system in z and $\overrightarrow{r}_{pnlCP}$ and $\overrightarrow{r}_{rotorOrg}$ are, respectively, the central point of the panel and the origin of the rotor.

The rigid velocity of each panel is related to the flapping and pitching motion of the blades, and can be expressed as

$$\overrightarrow{v}_{pitch} = (\dot{\theta}\, \overrightarrow{n}_{bladeCS,y}) \times (\overrightarrow{r}_{pnlCP} - \overrightarrow{r}_{bladeHinge})\,, \quad (13)$$

$$v_{flap} = (\dot{\beta}\, \overrightarrow{n}_{bladeCS,x}) \times (\overrightarrow{r}_{pnlCP} - \overrightarrow{r}_{bladeHinge})\,. \quad (14)$$

Where $\overrightarrow{n}_{bladeCS}$ refers to the axis of the blade local coordinate system, $\overrightarrow{r}_{bladeHinge}$ is the position of the hinge, $\dot{\beta} = d\beta/dt$ and $\dot{\theta} = d\theta/dt$.

The parameters that contribute to the velocity change in every iteration, thereby changing the panel velocity. So, the procedure described above has to be conducted in all iterations.

For the blade sections, the method is analogous, but it is considered the central point of each section instead of the central point of each panel.

With the right initial position of the helicopter, and the velocity of all the panels and section of the rotors, the program is ready to perform its first iteration.

D Thickness and Loading Noise Calculation

This section provides a description of how the thickness and loading noise are calculated and which parameters are involved on its calculation.

A detailed analysis of (4) revealed that the calculation of the thickness noise requires 16 variables for each panel, namely, the coordinates of the central point, the value of the total velocity in the actual and previous iterations, the panel area and the normal vector to the surface in the actual and previous iterations.

Through those variables, it is possible to obtain the value of the thickness noise for each panel as well as the time measured in the observer, which is the sum of the source time with the propagation time between the panel and the observer.

In the case of the loading noise calculation, first of all, the code must check if the blade azimuthal position is in the domain of the loading file. Then, it performs a linear interpolation of the load value if necessary and transforms the load values, in the rotor local coordinate system, into the global coordinates.

The calculation of the loading noise requires 16 variables for each section: the coordinates of the central points, the span and the total velocity and the load value in both the actual and previous iterations.

The calculation of the observer time of each section is similar to the one performed to the panels, considering the central point of the section.

E Microphone Noise

At this point, the value of thickness noise produced in each panel, the respective observer time and the loading noise value in each section and the instant it reaches the observer have all been determined.

The loading noise is calculated in the blade sections and the thickness noise in the blade panels, which originates different propagation times for the loading and the thickness noise. Moreover, for the same instant of the simulation, all panels present different values of observer time.

As a matter of fact, it is not the noise generated by each panel or section that is our objective, but the noise measured in the microphones. In order to obtain this value it is necessary to sum the contribution of all panels to obtain the thickness noise, and of all sections for the loading noise.

This operation raises several issues, being the most obvious one the process responsible for the noise summation, since all surfaces contribute at different instants of observer time. Besides the calculation of the total loading and thickness noise in each microphone, it is also necessary to calculate the total level of noise (sum of the thickness and loading noise) measured in each microphone. In other words, all panels and sections have to be conjugated in the same observer.

In order to solve those problems, the values of the thickness and loading noise have to be interpolated in the same observer time. All panels have different propagation times, so, in some instants of the simulation, only a few panels contribute to the noise. The same is true in the loading noise, but in the blade sections. The interpolation of the noise must start in the first instant in which all panels and sections contribute to the noise. That instant was denominated as t_{min} of the simulation.

The interpolations do not take place at a constant pace: to the same iteration, it has not been accomplished the same number of interpolations to all panels and sections. However, the total level of noise of a particular point in time can only be calculated if the noise generated by all the surfaces was already interpolated to that instant. One way to guarantee that all surfaces contribute to the interpolated instants is to perform the sum at the end of the simulation.

This seems to be a simple and efficient method, since it is guaranteed that all the interpolations contribute correctly to the sound spectrum. However, this method hides a big disadvantage, namely the required quantity of RAM. Therefore, instead of saving the data at the end of the simulation, the program will save it by segments of time, with a value specified by the user. These segments of time were denominated as windows.

F Acceleration of the Code - CUDA Programming

Now that the core of the program was presented, it is necessary to refer the role of the CUDA programming in the process.

To take full advantage of the processing computational power of the GPUs, it should be performed a large quantity of parallel calculations. After reviewing the different phases of the code, it was concluded that the calculation of the thickness noise for each panel and of the loading noise to each section was a good candidate to CUDA programming.

Both the loading and thickness noise demand a lot of intermediate calculations and all those calculations have to be repeated to all surfaces and microphones in each iteration.

The CPU performs those calculations in series: one microphone at a time, and for the same microphone, one panel/section at a time. It is easy to understand that a large portion of the overall time of the simulation is spent in this phase. Using the CUDA programming, those calculations can be performed simultaneously.

The device does not have access to the host data, so, all the data required to the noise calculation has to be transfered to the device. Then, the results have to be transferred back to the host.

The CUDA programming is more efficient when dealing with one-dimensional arrays, so, all variables which depend on the panel or section are saved into a single array.

The noise calculation does not require just the surfaces variables: it needs the coordinates of each microphone as well. For that reason, it was created another one-dimensional array containing the coordinates of all the microphones.

In order to storage efficiently the outputs, their values are placed in two one-dimensional arrays: one to the values obtained to the noise and another to the observer time in the microphones.

G Post-Processing

FACT is capable of generating three types of outputs with great importance in the noise analysis:

- The evolution of noise (thickness, loading and total) over time, measured in each microphone. The user can choose between the noise generated by all surfaces or just a specific rotor or blade;
- The magnitude of each harmonic frequency in the signal throughout the simulation in Pa, dB and dBA;
- The amplitude of each 1/3 octave band throughout the simulation, in dB and dBA.

These outputs can be obtained in any observer position(s) specified by the user or in a hemisphere of microphones above the rotorcraft.

IV. Results

This section presents two important results of FACT: the wind effect on the noise perceived at the observer and the advantage of GPU programming in terms of simulation speed.

A Wind Effect on Noise Perception

The results presented in this section are referent to a main rotor of a helicopter hovering over a hemisphere of 370 observer positions with a radius of $150m$. The rotor has no tilt, and it is in the centre of the hemisphere. Let us consider the wind, $\overrightarrow{W} = (40.93, 0.00, 4.30)m/s$, as represented in Fig. 2.

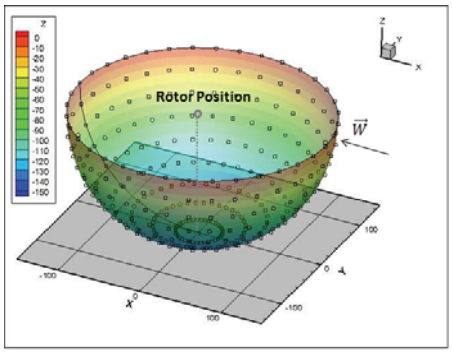

Fig. 2 Scheme of the rotor analysis

The results of thickness and loading noise (with and without wind) are represented, respectively by the hemispheres of Fig. 3 and Fig. 4 in dB and in Fig. 5 and Fig. 6 in dBA.

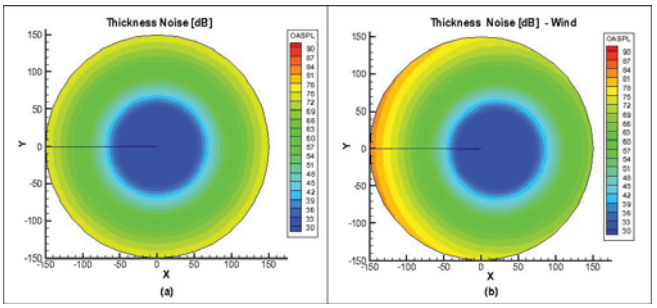

Fig. 3 1/3 octave bands of thickness noise in dB: (a) Without wind; (b) With wind

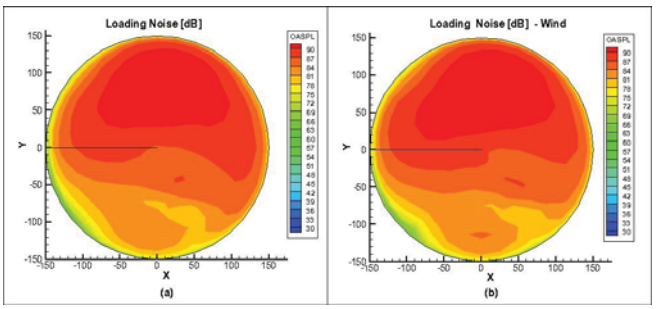

Fig. 4 1/3 octave bands of loading noise in dB: (a) Without wind; (b) With wind

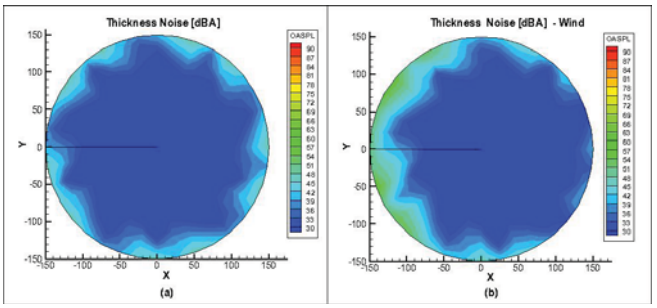

Fig. 5 1/3 octave bands of loading noise in dBA: (a) Without wind; (b) With wind

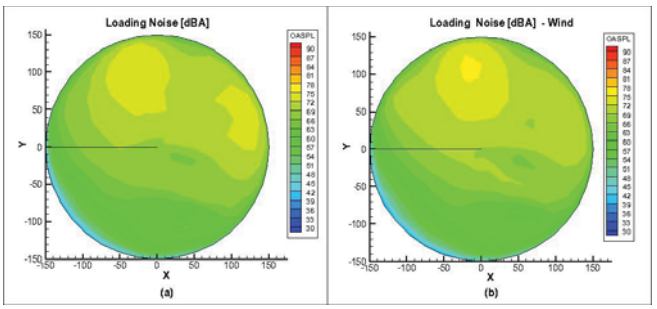

Fig. 6 1/3 octave bands of loading noise in dBA: (a) Without wind; (b) With wind

As expected, the thickness noise is higher in the positions aligned with the rotor and the loading noise has higher values below the rotor disk plane.

The introduction of wind affected the noise perceived at the observers both in the thickness and loading noise hemispheres: the noise footprint is slightly moved, with higher values in the wind direction.

All the results presented in this subsection were validated internally at CEIIA. The results correlation is not present for a question of confidentiality.

B CUDA Analysis

The present section will examine in which cases the application of the CUDA version of the code is advantageous comparatively to the original code. For this purpose, the same maneuver was used for all cases, with the lone exception of the blade mesh and the number of microphones, which will be modified.

In order to quantify the advantages of CUDA, the difference of the time spent on the total noise calculation using CUDA comparatively to the time spent with the original code to each case was calculated in terms of percentage.

TABLE I: Time of total noise calculation using CUDA in comparison with the normal code, in percentage

Mic \ Mesh	8x25	20x30	30x30	40x40
3	-508.33	-290.71	-149.10	-104.77
5	-223.46	-104.27	-78.95	-52.67
10	-140.12	-25.27	-10.84	20.23
15	-40.98	-11.40	22.12	35.71
20	-62.24	9.42	28.60	41.57
40	-3.06	39.20	46.99	52.15
60	16.78	48.09	50.73	54.12
80	28.90	51.81	54.40	–
100	33.98	52.79	–	–
120	38.79	53.79	–	-
160	45,62	–	–	–
200	47.40	–	–	–
300	53.41	–	–	–
400	57.29	–	–	–

The benefits of using CUDA are evident in this analysis, since the calculation of the total noise is approximately 50% faster in the most complex cases.

V. Quadrotor UAV Framework Analysis

Unmanned air vehicles are becoming indispensable in fields as infrastructure inspection, agriculture, search, rescue and reconnaissance missions, only to name a few.

The growing number of UAV applications led to the first concerns regarding more silent configurations, not only because of its environmental impact, but also as a mission requirement, in case of military and police applications. Rotating surfaces, as propellers and rotors, are usually the dominant source of noise in UAVs, especially in the case of quadrotor.

In light of this, CEIIA and UAVision are cooperating in order to find more silent UAV configurations to reduce acoustic footprint even further. The first test study will be the quadrotor UX-SPYRO of UAVision (Fig. 7).

Fig. 7 UX-SPYRO quadrotor UAV

UAV quadrotor noise is new area of research, and the computational procedure presented before and validated for helicopters must also be validated for this type of vehicle due to its distinct characteristics, as a reduced rotor area, lower angular speed (and subsequent lower Reynolds number) and higher rotor interaction when compared with helicopters.

In the absence of experimental data, a framework for the validation and subsequent noise optimization was created, represented below, in Fig. 8.

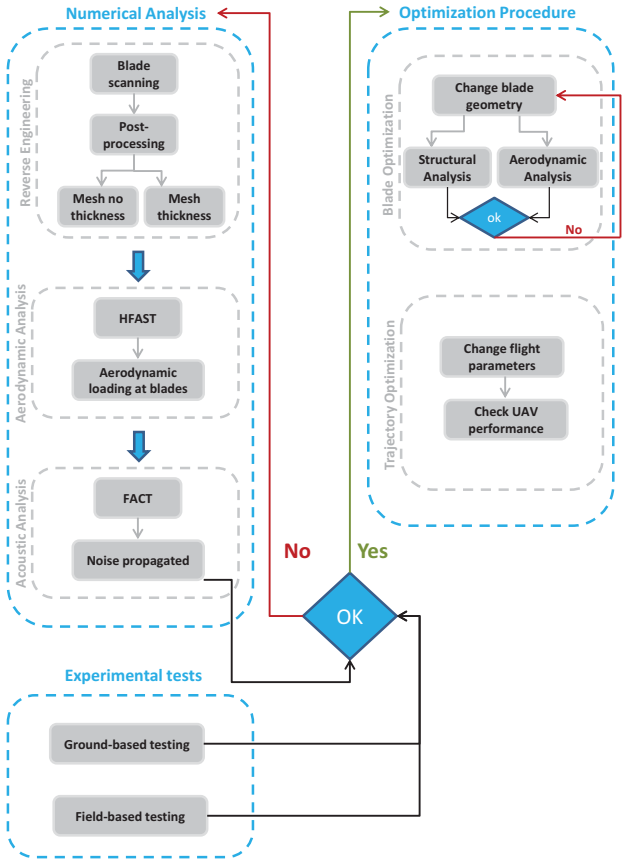

Fig. 8 Quadrotor UAV framework for acoustic analysis

The following two subsections describe the experimental setup for the ground-based and field-based testing, that is

being used for the validation of the computational chain HFAST+FACT for quadrotor UAVs.

A Ground-based Testing

The objective of the ground-based testing is to measure the noise propagation in a controlled environment in order to help validating the aeroacoustics simulation of a single rotor of the UAV.

These measurements will be performed in the anechoic room of IST's aero-acoustic tunnel (represented in Fig. 9).

Fig. 9 IST's anechoic room

This experimental procedure comprises two main challenges:

1) **Identify the dominant type of noise:**
   FACT is capable of calculating the thickness and loading noise separately, i.e., it is possible to find which type of noise is more significant. These two different types of noise have different nature and directions of propagation and with the right experimental setup it is possible to determine the parameters that influence the acoustic behaviour the most.
2) **Study the influence of engine noise:**
   In the case of a quadrotor, engine noise is less significant than rotor noise; however, its influence can still affect the measurements, and for that reason it is important to be able to isolate the engine noise.

Different sets of measurements will be conducted, in the rotor plane and below the rotor plane, at different relative distances to the centre of the rotor, for different values of angular speed.

B Field-based Testing

The aim of this analysis is to correlate the real noise propagated by the UAV during flight with the values calculated with FACT.

It will also be an opportunity to identify possible sources of discrepancies and their specific impact, such as atmospheric and reflection effects and interaction between rotors and rotors and fuselage.

The field-based measurements will take place at UAVision facilities, where the UAV flight tests are usually conducted. These experimental measurements must be conducted in the best atmospheric conditions possible.

Three different flight conditions will be considered:

- Hover;
- Take-off;
- Landing.

Similarly to the ground-based testing, the sound level meter position would be changed in order to acquire enough data to the numerical analysis correlation, as represented in Fig. 10.

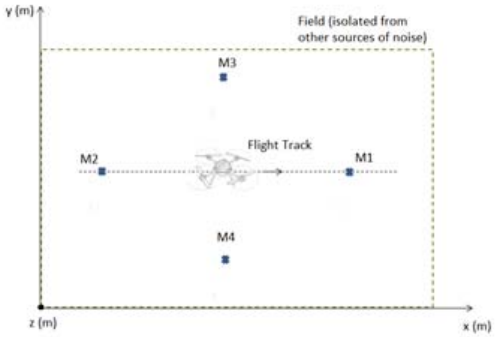

Fig. 10 Scheme of flight noise measurements

VI. Conclusion

This paper describes the development of an acoustic tool capable of predicting the thickness and loading noise generated during the helicopter flight.

The new acoustic tool was built in a way that enables several rotorcraft configurations and addresses its full movement, steady and unsteady, with wind as atmospheric condition.

The advantage of GPU programming is clearly evident, allowing the simulation of complex analysis in short time.

The new acoustic tool was validated for helicopters and an experimental procedure for quadrotor UAV noise is being conducted in order to validate CEIIA's computational chain for this type of emerging vehicles.

In the scope of this project, further work is being carried out in the following activities:

- Correlation of numerical analysis with experimental data from rotor noise measurements in a controlled environment;
- Correlation of numerical analysis for UAV quadrotor maneuvering noise;
- UX-SPYRO quadrotor noise footprint optimization;
- Implementation of noise predition in transonic conditions in FACT;
- Implementation of noise scattering in FACT.

References

[1] Ffowcs Williams J.E. and Hawkings D.L. Sound Generation by Turbulence and Surfaces in Arbitrary motion. *Mathematical and Physical Sciences*, 264(1151):321–342, May 1969.

[2] Farassat F. The Kirchhoff Formulas for Moving Surfaces in Aeroacoustics - The Subsonic and Supersonic Cases. Technical Memorandum 110285, NASA, Langley Research Center, Hampton, Virginia, September 1996.
[3] F. Farassat. Derivation of Formulation 1 and 1A Farassat. Technical report, NASA, March 2007.
[4] Brès G.A., Brentner K.S., Perez G., and Jones H.E. Maneuvering rotorcraft noise prediction. *Journal of Sound and Vibration*, 275:719–738, 2004.
[5] Brentner K. S., Brès G. A., G. Perez, and Jones H. E. Maneuvering Rotorcraft Noise Prediction: A New Code for a New Problem. Technical report, In Proceedings of AHS Aero- dynamics, Acoustics, and Test and Evaluation Technical Specialists Meeting, San Francisco, CA, January 2002.
[6] Ianniello S. Algorithm to Integrate the Ffowcs Williams-Hawkings Equation on Supersonic Rotating Domain. *AIAA*, 37(9):1040–1047, September 1999.
[7] Brentner K. S. and H.E. Jones. Noise Prediction For Maneuvering Rotorcraft. Technical report, NASA, 2000.
[8] Perez G., Brentner K. S., Brès G. A., and Jones H. E. A First Step Toward the Prediction of Rotorcraft Maneuver Noise. *Journal of the American Helicopter Society*, 50(3):203–237, July 2005.
[9] Hsuan-nien C. *Rotor noise in maneuvering flight*. PhD thesis, The Pennsylvania State University, The Graduate School, December 2006.
[10] Brentner K. S., Burley C. L., and Marcolini M. A. Sensitivity of Acoustic Predictions to Variation of Input Parameters. *Journal of the American Helicopter Society*, 39(3):43–52, July 1994.

Ana Vieira is an aeroacoustics researcher engineer at CEIIA. She attended IST (Instituto Superior Técnico) from 2007 to 2013 and holds a Master's Degree from this institution.

Fernando Lau obtained his PhD in Aeroacoustics at Instituto Superior Tecnico, Universidade de Lisboa, where he is currently an Assistant Professor. His main research interests are Aeroacoustics, Morphing structures and Aircraft Design Optimization.

João Pedro Mortágua is currently the head of CEIIA's R&D Unit. In his past, João Pedro led CEIIA's Aeronautical Unit for several years, having been strongly involved in the establishment of CEIIA as a player in this market. João Pedro holds a double MSc degree in Aerospace Engineering from Delft University of Technology and from Lisbon's Instituto Superior Técnico. In his extensive professional experience, he has worked as a Project Manager for AIRBUS, EMBRAER and TAP. He was, as well, a researcher at NASA -Dryden Flight Research Centre.

Luís Cruz is an aeroacoustics engineer at CEIIA working as subcontractor for AgustaWestland UK developing tools and methods for helicopter aeroacoustic predictions. He graduated with a MSc in aerospace engineering in 2009 at Instituto Superior Técnico in Lisbon, Portugal. He joined the AgustaWestland Rotor Aerodynamics department in 2010 and initially he was involved in developing a new acoustic optimization framework aimed at minimizing helicopter on-ground noise footprint. More recently he has been developing a new set of aeroacoustic tools based on the CUDA framework to massively accelerate and expand the aeroacoustic analysis capabilities.

Rui Santos received two M.S. degrees, in Mechanical Engineering and Engineering Design from Instituto Superior Técnico, Lisbon, in 2001 and 2004, respectively. He is currently working as a Research Program Manager at the Center for Innovation, Technology and Policy Research IN+, at Instituto Superior Técnico. His research interests lie in the areas of Aeroacoustics, Vibro-Acoustics, Composites and Metal Additive Manufacturing.